Supersonic Propagation of an Ionization Front in Low Density Foam Targets Driven by Thermal Radiation

T. Afshar-rad,[1] M. Desselberger,[1] M. Dunne,[1] J. Edwards,[1,*] J. M. Foster,[2] D. Hoarty,[2] M. W. Jones,[1] S. J. Rose,[3] P. A. Rosen,[2] R. Taylor,[1] and O. Willi[1]

[1]*Imperial College of Science, Technology and Medicine, London, SW7 2BZ, United Kingdom*
[2]*Atomic Weapons Establishment, Aldermaston, Reading, United Kingdom*
[3]*Rutherford Appleton Laboratory, Chilton, Didcot, United Kingdom*

(Received 24 March 1994)

Observations of the sustained propagation of a supersonic ionization front, produced by an intense pulse of thermal radiation in low density foam targets, are reported. The position of the front was observed with a high resolution soft x-ray imaging system (at 50 and 70 Å), using 1D continuous streaks and 2D gated images. The experimental observations were in good agreement with 1D and 2D radiation hydrodynamic code simulations.

PACS numbers: 52.25.Nr, 52.50.Jm

The investigation of supersonic heat wave propagation in matter driven by thermal radiation is of fundamental interest in the study of radiation hydrodynamics in both laboratory and astrophysical plasmas. Examples can be found in the dynamics of gaseous nebulae and in the formation of ablation fronts as the intense radiation field from a hot star interacts with a remote interstellar cloud [1]. In addition there may be important terrestrial applications in laser driven inertial confinement fusion (ICF), where the preforming of a plasma buffer could act to thermally smooth laser nonuniformities before they reach the ablation surface of an implosion capsule [2]. The production of this buffer through the passage of a supersonic x-ray driven wave would avoid the formation of preheating shocks which would otherwise result from the high x-ray intensities needed to form the required plasma scale lengths [3]. The implosion will thus be allowed to proceed along a lower adiabat. The propagation of radiatively driven supersonic ionization fronts is also of interest in ion-beam ICF, where the process may provide a means of decoupling the implosion process from nonuniform beam irradiation [4].

Several studies have recently been carried out to investigate the interaction and heating of thin solid targets with intense, quasi-Planckian soft x-ray pulses. These experimental observations measured global radiation transport [5,6], shock propagation [7], opacities [8,9], the propagation of Marshak waves [10], and the acceleration dynamics of thin foil targets [11]. In these measurements the initial propagation of the heat wave is supersonic but is rapidly overtaken by the hydrodynamic motion and the flow soon becomes ablative [12]. A supersonic heat wave can, however, be maintained by lowering the target density. The recent development of sufficiently uniform, low density polymer foams has provided a suitable target material for use in such experiments.

In this Letter we report on direct measurements of the sustained propagation of a supersonic, radiation driven heat wave. A cylindrical low density foam target was irradiated by soft (<1 keV) x rays from a spatially separate gold converter foil. The position of the ionizing heat front in this foam target was observed using a high resolution, soft x-ray, side-on radiographic imaging system using 2D gated and 1D streak detectors. This side-on detection system allowed the temporal development of the ionization wave to be studied. The experiment was modeled with 1D and 2D Lagrangian radiation hydrodynamics codes, resulting in good agreement. The supersonic nature of the ionization front was sustained for many hundreds of picoseconds, with the reemission of x rays in the heated target shown to play a crucial role in the dynamics of the front.

Seven frequency-doubled ($\lambda = 0.53$ μm) beams from the VULCAN glass laser system at the Rutherford Appleton Laboratory were used in a cluster arrangement (with a cone angle of 13° including a beam at the center of the cone) to irradiate a thin gold layer, 1500 Å thick, supported on a 1 μm plastic substrate. The soft x-ray pulse transmitted through the rear of this converter foil was used to irradiate a low density foam target, separated from the foil to ensure only x-ray heating of the foam occurred. This separation was set at 30 μm and was monitored using a pair of high magnification telescopes, accurate to within 10 μm. The pulse had a full-width-half-maximum (FWHM) duration of typically 1300 ps and was focused to a focal spot of approximately 250 μm diameter, producing laser irradiances of around 1×10^{15} W cm^{-2}. The geometry is shown schematically in Fig. 1. The foam samples used were primarily triacrylate ($C_{15}H_{20}O_6$) chemically doped with a chlorine monomer ($C_9H_3O_2Cl_5$) to 25% by weight chlorine. These cylindrical targets had a diameter of 160 μm and lengths of up to 200 μm, at a density of 50 mg/cm^3 (approximately 1/30th solid density), and were oriented so that the flat face of the cylinder faced the gold converter foil. Cell sizes in the foam were less than 1 μm in diame-

0031-9007/94/73(1)/74(4)$06.00

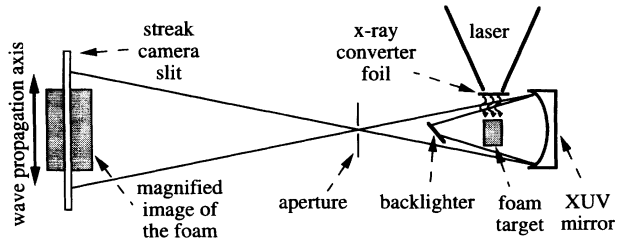

FIG. 1. A schematic of the target and imaging geometry.

ter, with a very high degree of homogeneity throughout the foam [13]. This was confirmed through the use of off-line, point source x radiography and scanning electron microscopy [14]. The temporal behavior and the absolute flux levels of the soft x-ray pulse produced from the gold converter foil were measured with a temporal resolution of better than 100 ps using a calibrated, flat response vacuum x-ray diode. A rear side x-ray conversion efficiency of $(4 \pm 1.5)\%$ was observed, in agreement with previous measurements. This indicated an x-ray flux incident on the foam sample of $(3.8 \pm 1.4) \times 10^{13}$ W cm^{-2} (equivalent to a blackbody temperature of 138 ± 12 eV). The optical burnthrough of the gold converter foils was monitored on separate shots to ensure that the drive foil remained supercritical throughout the experiment. It was confirmed that the burnthrough occurred late in time (after 1500 ps), well after all the wave propagation measurements, which were taken on the rising edge of the x-ray pulse. Additional experiments were performed in which lower x-ray fluxes and varying levels of chlorine dopant were used, providing scaling characteristics of the wave propagation with drive flux and average Z, as will be discussed in a forthcoming publication.

The foam target was backlit by a soft x-ray source and imaged perpendicularly to the soft x-ray drive with a spherical multilayered mirror, as previously described [15]. For the chlorinated foams examined in the current study, the mirrors were coated to reflect at a central wavelength of 70 Å (175 eV), with a bandwidth measured to be better than ± 5 Å. In this spectral region the dominant contribution to the radiative opacity is bound-free absorption, with no contribution from bound-bound transitions, as confirmed using extreme ultraviolet absorption spectroscopy. A 50 times magnified image of the cylindrical target was produced and recorded either on the slit of a soft x-ray streak camera to provide continuous 1D information or on a two frame gated microchannel plate (MCP) intensifier with the target image placed across the two frames. This allowed information on the 2D response of the target to be monitored. The spatial resolution of the imaging system was found to be less than 1 μm by the use of a ray tracing program which modeled the specific target geometry adopted, although the actual measured resolution in the streaked images was around 5 μm, limited primarily by photocathode noise. The streak camera spatially integrated over an area ± 7 μm about the foam's axis. Over this region the difference in path lengths for rays traversing different chords of the cylinder is negligible. The temporal resolution of the streak camera was 50 ps and the gating time of the x-ray imager was approximately 120 ps.

A radiogram of a chlorinated foam target subjected to an intense radiation field is shown in Fig. 2, demonstrating the evolution of the ionization wave as it propagates into the undisturbed foam. At early time, the foam is opaque to the monochromatic probe radiation since it is cold and un-ionized, allowing the backlighter to be seen only in front of and behind the cold target. The converter foil also obscures the backlighter, allowing only a thin band of backlighter signal to appear on the front side of the foam at early time. As the x-ray drive pulse turns on the opacity of the foam is reduced, so allowing the probing x rays to pass through deeper into the target. For a target density of 50 mg/cm^3 and a probe wavelength of 70 Å, the chlorinated foam is calculated to become 50% transparent at an electron temperature of 80 eV, using the detailed configuration accounting opacity code, IMP [16]. The 50% transmission contour will be taken as being representative of the position of the ionization front. The initial velocity of this contour (essentially the 80 eV contour since there is little perturbation of the target density), 300 ps after the start of the x-ray drive is $(3.5 \pm 0.5) \times 10^7$ cm/s. This velocity remains above 1.3×10^7 cm/s throughout the measurement. For these conditions, the maximum possible sound speed in the heated material is 10^7 cm/s, as discussed below.

In order to further assess the heating characteristics of the radiation field, 2D gated images were taken at various times in the evolution of the ionization front. A range of foam targets was studied, with one example displayed in Fig. 3. This shows images taken at 300 and 900 ps after the start of an x-ray pulse which irradiated an undoped (pure triacrylate) foam of density 30 mg/cm^3. For this

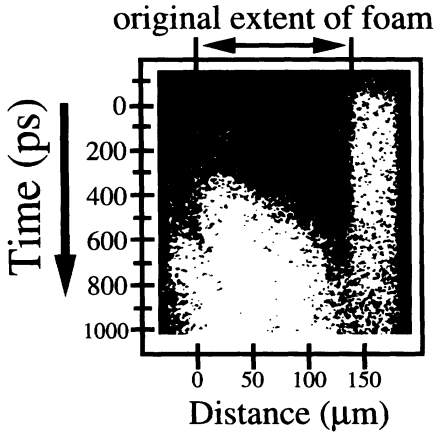

FIG. 2. Soft x-ray (70 Å) streaked radiogram of a 50 mg/cm^3, 135 μm long triacrylate foam with a 25% by weight chlorine dopant. The x-ray drive is incident from the left. The probe starts 100 ps before the arrival of the drive radiation, allowing the original extent of the target to be monitored. The passage of a supersonic ionization front is evidenced by the evolution of the transmission of the foam target.

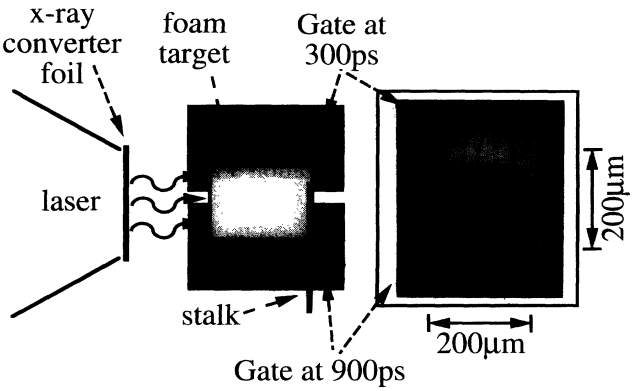

FIG. 3. Soft x-ray (50 Å) gated radiograms showing the 2D response of a 30 mg/cm^3 undoped triacrylate foam target to the passage of a supersonic, radiatively driven ionization front. The image of the foam target straddles the two time frames. The geometry is shown schematically to the left. As in Fig. 2, the light areas in the print arise from the unattenuated probe radiation, while the dark areas correspond to absorption by the unheated foam.

image the foam was separated from the converter foil by 125 μm, producing a slightly lower drive irradiance and consequently reduced propagation velocity. This velocity still remains well above the sound speed due to the concomitant reduction in the ambient plasma temperature. In the early time frame, the foam target remains relatively undisturbed since the drive was just starting to rise. At later time, however, the ionization wave can be seen to have penetrated deep into the target (having traveled 60 μm in no more than 600 ps), with a high degree of spatial uniformity. An important point to note is that the diameter of the foam target at the position of the ionization front remains unchanged from its original value. This is an indication of the supersonic nature of the propagation and the consequent lack of significant material compression behind the front. Measurements taken at lower x-ray drive irradiances (approximately 10^{12} W cm^{-2}), in which the heat front is preceded by a shock front, resulted in a "rolling up" of the foam at the position of the shock front.

Simulations were performed using both the 2D Lagrangian radiation hydrodynamics code, NYM [17] in which radiation transport was modeled using a multigroup implicit Monte Carlo (IMC) technique [18], and a 1D Lagrangian radiation hydrodynamics code [5] modified to take account of the geometrical coupling between the extended source and the sample. The temporal behavior and absolute levels of the x-ray drive were taken from the calibrated diode measurements, with the spectrum of the radiation assumed to be a blackbody defined by the ambient radiation flux. The use of this blackbody assumption has been shown to result in good agreement with experimental data in previous measurements where a similar converter foil geometry was used [5]. The drive spectrum was altered to take account of long mean-free-path x rays originating from the gold M, N, or O bands, but this was found to have only a small effect on the wave propagation characteristics. The effect of electron thermal conduction was found to be insignificant except at very early time. Opacities were calculated from tabulated values generated using the detailed configuration accounting opacity code, IMP. Very similar results were obtained with the 1D code compared with the full 2D calculations, as may be expected if the supersonic nature of the radiation flow allowed a simple heating wave to propagate well ahead of any hydrodynamic response of the target. A comparison of the measured and predicted propagation of the 50% transmission point of the data shot shown in Fig. 2 can be found in Fig. 4. The simulated foam transmission curves were obtained by postprocessing the output of the hydro simulations with opacities generated from IMP. Good agreement on the extent and speed of propagation of the x-ray heating wave can be observed at all times in the evolution of the front. It was essential in these simulations to include target reemission in the transport equations. The effect of neglecting this reemission in the 1D simulations can be seen in Fig. 4 (curve C).

When an intense radiation field is incident onto cold matter, the radiation penetrates about a photon mean free path into the material, which is consequently heated and ionized. The region where the unheated, un-ionized material is transformed into an ionized plasma defines an ionization front. If the x-ray flux is sufficiently high and the

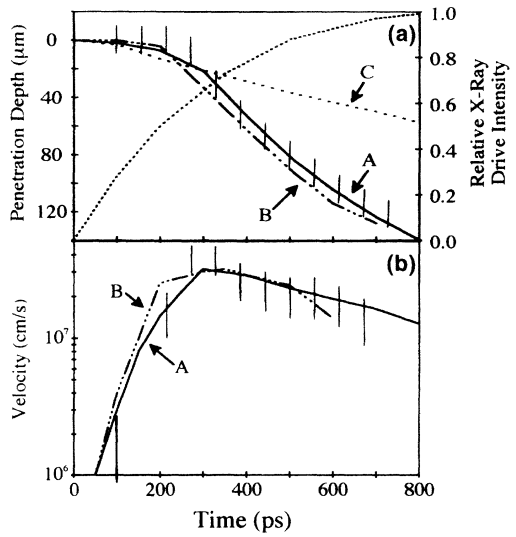

FIG. 4. (a) A comparison of the observed and calculated propagation characteristics of the ionization wave observed in Fig. 2. The experimentally measured propagation of the 50% transmission point (vertical bars) includes errors arising primarily from noise in the backlighter signal. Radiation hydrodynamics code predictions in 1D (curve A) and 2D (curve B) match the experimental well. The effect of allowing the target reemission to escape without contributing to the driving of the ionization front is shown in curve C. Also shown is the measured x-ray pulse shape. (b) Velocities of the 50% transmission contour from the experiment (vertical bars) and the 1D (curve A) and 2D (curve B) simulations.

material density sufficiently low, as in the situation presented here, the propagation of such an ionization front can outrun any hydrodynamic motion which results from the large pressure differential between the heated and unheated material. That is, the upstream and downstream material in the region of the front can coexist at the same density despite the presence of large temperature and pressure gradients. The front is said to propagate supersonically with respect to both the heated and unheated matter. The development of global hydrodynamic motion in the plasma can be characterized by the ion sound speed, for which an upper estimate may be obtained by assuming a plasma temperature equal to the maximum x-ray drive temperature and ignoring reductions due to nonideal gas behavior. For the present conditions, this maximum possible sound speed is 10^7 cm/s, which is well below the propagation velocities observed. In reality any shock wave will propagate at lower velocities, primarily since the ambient plasma temperature will never reach the drive temperature due to the relatively low target Z. Even assuming this maximum sound speed, however, the ionization wave in the foam propagates supersonically for at least 600 ps. This situation is reproduced in the simulations, which predict that density disturbances only catch up to the heat front after 1 ns. A time sequence of temperature and density profiles in the foam target taken from the 1D simulations is shown in Fig. 5. This demonstrates the heat wave extending beyond the hydrodynamic motion which takes the form of a weak, ablative compression wave propagating behind the radiation heat front. The weak density disturbances seen at the position of the front can be understood from classical radiation hydrodynamics. If, for simplicity, we assume isothermal equilibrium in the downstream plasma then the density jump should be given approximately by $1 + (a/u)^2$, where a is the sound speed in the heated material and u is the velocity of the ionization front. Taking the upper limit imposed on the sound speed and the measured propagation velocity of 3.5×10^7 cm/s, a final downstream density of 55 mg/cm^3 is obtained, in agreement with the radiation hydrodynamics code predictions. The production of a supersonic radiation heat front

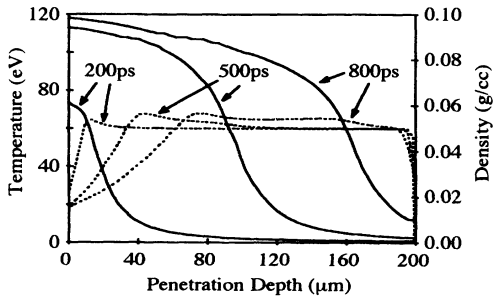

FIG. 5. Calculated temperature (solid line) and density (dashed line) profiles in the foam target at three stages in the passage of the ionization front. The drive is incident from the left. The temperature wave can be observed to penetrate deep into the unshocked foam.

under these conditions can be readily understood by noting that the radiative flux (σT^4) is at least 7.5 times larger than the hydrodynamic energy flux (ρa^3).

In summary, we have observed the propagation of a sustained, supersonic ionization wave driven by thermal radiation for the first time in the laboratory. The side-on radiography technique adopted permitted a study of both the spatial extent and uniformity of the wave front and the evolution of the velocity of the wave. The data were well reproduced by 1D and 2D Lagrangian radiation hydrodynamics codes, which showed target reemission to play a major role in the transport characteristics of the radiation wave.

Apart from its intrinsic interest, the technique of supersonically forming such plasmas may prove to be important in the elimination of laser nonuniformity imprint in the initial phase of laser driven implosions. It should be possible to tailor the size of the preformed, supercritical plasma to smooth the dominant laser nonuniformities while still allowing the production of high ablation pressures [3].

The authors would like to acknowledge the technical support of the CLF laser and target area staff, B. Evans (University of Reading) for supplying the multilayered mirrors, C. Horsfield (AWE), W. Nazarov, and J. Falconer (Dundee University) for supplying the foam targets. Thanks are also due to C. Smith (AWE) for valuable comments and assistance. This work was jointly funded by the SERC and MoD.

*Presently employed at AWE Aldermaston, Reading, United Kingdom.

[1] W. I. Axford, Philos. Trans. R. Soc. London A **253**, 301 (1961).
[2] M. Desselberger *et al.*, Phys. Rev. Lett. **68**, 1539 (1992).
[3] M. Desselberger, M. Jones, J. Edwards, M. Dunne, and O. Willi (to be published).
[4] A. R. Piriz and S. Atzeni, Plasma Phys. Controlled Fusion **35**, 451 (1993).
[5] J. Edwards *et al.*, Phys. Rev. Lett. **67**, 3780 (1991); J. Edwards *et al.*, Europhys. Lett. **11**, 631 (1990).
[6] W. Schwanda and K. Eidmann, Phys. Rev. Lett. **69**, 3507 (1992).
[7] T. Endo, H. Shiraga, K. Shihoyama, and Y. Kato, Phys. Rev. Lett. **60**, 1022 (1988).
[8] T. S. Perry *et al.*, Phys. Rev. Lett. **67**, 3784 (1991).
[9] J. Foster *et al.*, Phys. Rev. Lett. **67**, 3255 (1991).
[10] R. Sigel *et al.*, Phys. Rev. Lett. **65**, 587 (1990).
[11] J. Edwards *et al.*, Phys. Rev. Lett. **71**, 3477 (1993).
[12] N. Kaiser, J. Meyer-teh-Vehn, and R. Sigel, Phys. Fluids B **1**, 1747 (1989).
[13] J. Falconer *et al.*, J. Vac. Sci. Technol. A **8**, 968 (1990).
[14] C. Horsfield, AWE Aldermaston (private communication).
[15] M. Desselberger *et al.*, Appl. Optics **30**, 2285 (1991); O. Willi *et al.*, Rev. Sci. Instrum. **63**, 4818 (1992).
[16] S. Rose, J. Phys. B **25**, 1667 (1992).
[17] P. D. Roberts, AWE report, 1980 (unpublished).
[18] J. A. Fleck and J. D. Cummings, J. Comput. Phys. **8**, 313 (1971).

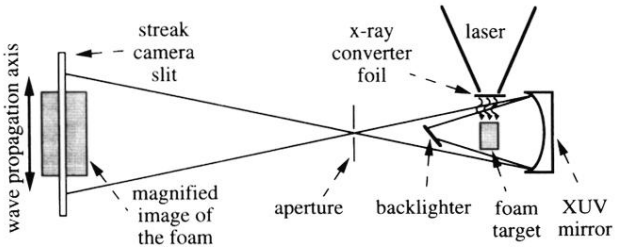

FIG. 1. A schematic of the target and imaging geometry.

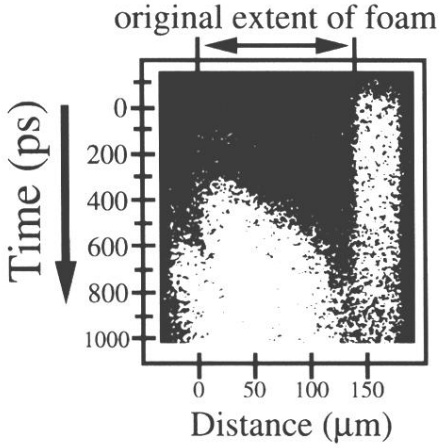

FIG. 2. Soft x-ray (70 Å) streaked radiogram of a 50 mg/cm^3, 135 μm long triacrylate foam with a 25% by weight chlorine dopant. The x-ray drive is incident from the left. The probe starts 100 ps before the arrival of the drive radiation, allowing the original extent of the target to be monitored. The passage of a supersonic ionization front is evidenced by the evolution of the transmission of the foam target.

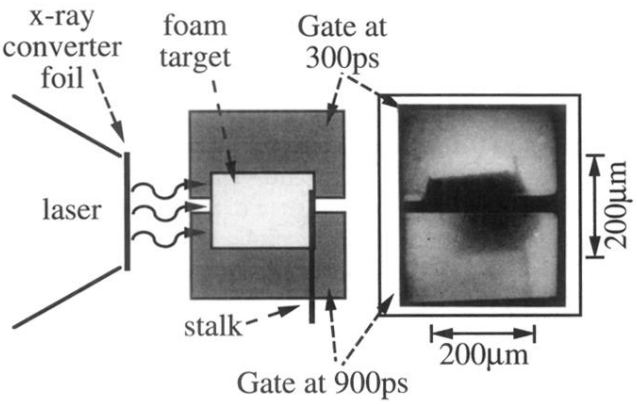

FIG. 3. Soft x-ray (50 Å) gated radiograms showing the 2D response of a 30 mg/cm^3 undoped triacrylate foam target to the passage of a supersonic, radiatively driven ionization front. The image of the foam target straddles the two time frames. The geometry is shown schematically to the left. As in Fig. 2, the light areas in the print arise from the unattenuated probe radiation, while the dark areas correspond to absorption by the unheated foam.